Simulation of Near-field Photolithography Using Finite-difference Time-domain Method

Simulation of near-field photolithography using the finite-difference time-domain method

Shuji Tanaka[a)] and Masayuki Nakao
Department of Engineering Synthesis, The University of Tokyo, 7-3-1 Hongo, Bunkyo-ku, Tokyo 113-8656, Japan

Mariko Umeda and Kenchi Ito
Central Research Laboratory, Hitachi Ltd., 1-280 Higashi-Koigakubo, Kokubunji-shi, Tokyo 185-8601, Japan

Shigeru Nakamura
Digital Medea Products Division, Hitachi Ltd., 1410 Inada, Hitachinaka-shi, Ibaragi 312-8505, Japan

Yotaro Hatamura
Department of Engineering Synthesis, The University of Tokyo, 7-3-1 Hongo, Bunkyo-ku, Tokyo 113-8656, Japan

Illuminating a transparent mold under total internal reflection condition generates evanescent light. Near-field photolithography uses such light, and we simulated this exposure in two dimensions using the finite-difference time-domain (FDTD) method. Our simulation suggests the feasibility of resolving a 130 nm pitch grating pattern, which is finer than the diffraction limit of light. The simulation results showed fair agreement with our experimental results, confirming the strong influence of exposure light polarization to the distribution of optical near fields in photoresist films. This indicates that the FDTD simulation is promising to predict exposure results for designing molds. We further extended the simulation varying the thickness and refractive index of a photoresist film. Based on the simulation results, showing the good exposure contrast in the thin surface layer of the photoresist film, we suggested two methods to resolve a thick resist film: the multilayer resist method which allows us to use a sufficiently thin photoresist film, and the surface imaging technology which can completely dry develop a thick photoresist film even if its exposure area is confined in the surface layer. © *2001 American Institute of Physics.*
[DOI: 10.1063/1.1351866]

I. INTRODUCTION

A scanning near-field optical microscope (SNOM) realizes spatial resolution finer than the diffraction limit of light by using near-field light which is generated by illumination under total internal reflection condition or through an aperture smaller than the light wavelength. This high resolution served by such near-field light has led to studies for applying it to microfabrication. Mitsuoka *et al.*[1] fabricated 100 nm wide grooves, which are narrower than the diffraction limit of light, on a photoresist film by scanning near-field light with a wavelength of 442 nm generated at the tip of a sharp optical-fiber-based SNOM probe. Ono and Esashi,[2] Alkasi *et al.*,[3] and Goodberlet[4] experimentally confirmed that conformal contact photolithography using near-field light can transfer photomask patterns finer than the exposure light wavelength to photoresist films. Alkasi *et al.* used broadband UV light from a mercury arc lamp to fabricate a 140 nm pitch grating pattern. McNab and Blaikie[5] investigated light intensity contrast in the optical near field of subwavelength period gratings using the multiple multipole technique. Other reports include methods using an elastomeric phase mask,[6] an elastmeric light-coupling mask,[7] and a solid immersion lens.[8]

In our former article,[9] we reported near-field photolithography to accomplish resolution higher than the diffraction limit of light by using a transparent mold with a microrelief which is illuminated under total internal reflection condition. Further study revealed, however, the complicated nature of the exposure which sometimes produces photoresist patterns different from microrelief patterns on the mold; an example is the dependence on the illumination direction found in the different widths of groove pairs fabricated on a photoresist film, whereas the pair of ridges on the mold were of the same size.

To better understand such complicated nature of the exposure and theoretically model our near-field photolithography process, we applied the finite-difference time-domain (FDTD) method to calculate optical near-field distribution in photoresist films. FDTD method is promising for simulating optical near fields, as already proven in many calculations of optical near-field distribution at the end of SNOM probes. This article explains our FDTD simulation and compares the simulation results with experimental results.

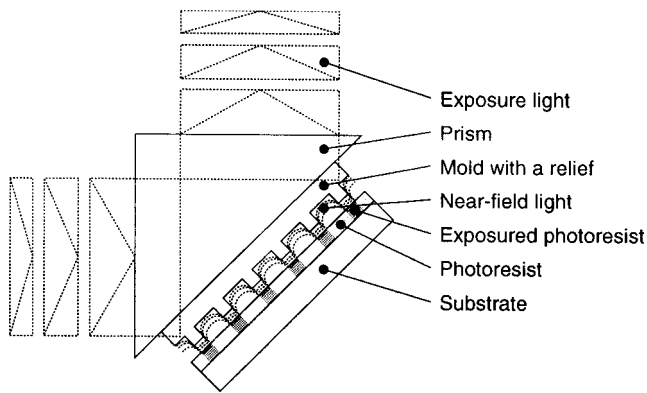[a)]Electronic mail: shuji@cc.mech.tohoku.ac.jp

FIG. 1. Exposure method of the near-field photolithography. The transparent mold with the microrelief is illuminated under total internal reflection condition. The photoresist film is exposed to evanescent light generated in the near field of the mold surface.

II. EXPOSURE METHOD AND PROCESS OF THE NEAR-FIELD PHOTOLITHOGRAPHY

Figure 1 illustrates the exposure method of near-field photolithography. A transparent mold with microrelief is used in place of a conventional photomask. The mold is located close to a photoresist film at a distance much smaller than the exposure light wavelength, and is illuminated through a prism under total internal reflection condition. The photoresist film is exposed to near-field light modulated by the microrelief on the mold. The near-field light, including evanescent light, decays exponentially with a distance from the mold surface. Therefore, exposure of the photoresist film facing the protruding part of the micorelief is much stronger than that facing the bottom part, and a feature defined by the microrelief is transfered into the photoresist film. Note that the near-field light contains high spatial frequencies modulated by microrelief structures finer than the diffraction limit of light, producing a spatial resolution beyond the diffraction limit of light.

For practical near-field exposure, the mold contacts the photoresist film, because a constant gap on the order of nanometers between the mold and the photoresist cannot be kept due to the imperfect flatness of the mold and photoresist film surface. Thus, the mold has to follow the surface of the photoresist for the contact. The mold also has to be replaced at low cost when damaged by contact with the photoresist film. Therefore, we replicated a hard master mold using flexible transparent plastic, and the flexible replica molds were used for the exposure. For our experiment, we replicated a silica glass master mold, which was fabricated by electron beam lithography and fast atom beam etching, using acetyl cellulose films.

III. SIMULATION MODEL

Using the two-dimensional FDTD method, we calculated the distribution of optical near-field intensity in photoresist films exposed by the method illustrated in Fig. 1. The two-dimensional calculation cannot handle some cases like when the exposure light is incident parallel to linear ridges on the mold, however, it saves computing time and resource.
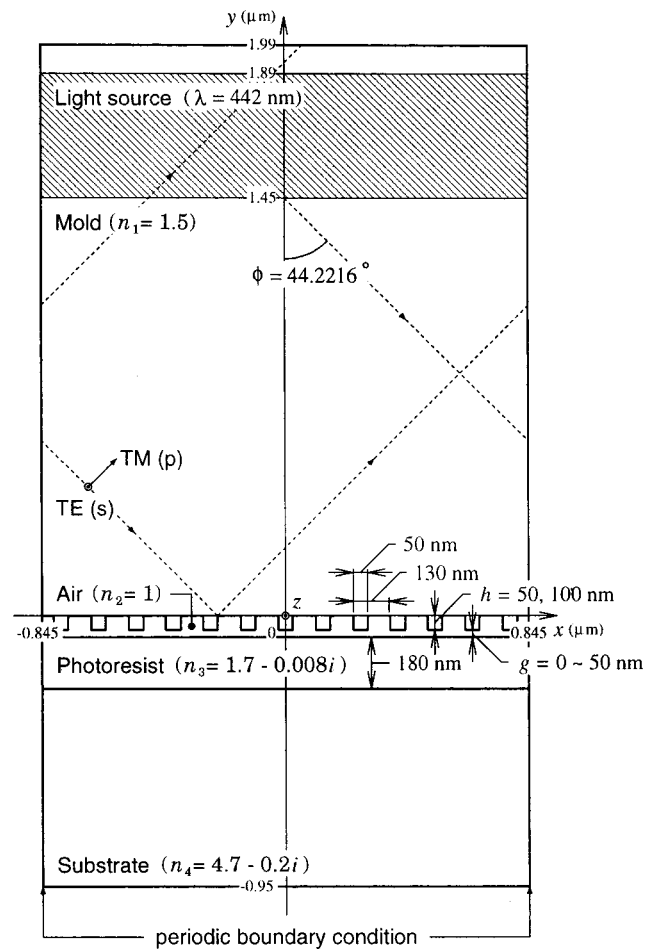

FIG. 2. Simulation model for the FDTD method. The refractive indices of the mold, the air, the photoresist and the silicon are $n_1 = 1.5$, $n_2 = 1$, $n_3 = 1.7 - 0.008i$, and $n_4 = 4.7 - 0.2i$, respectively. At the right and left boundaries of the simulation model, periodic boundary conditions are introduced.

Figure 2 shows a 1.69×2.94 μm simulation model consisting of a mold, an air gap, a photoresist film, a silicon substrate and a light source. The refractive indices of the mold, the air, the photoresist and silicon are $n_1 = 1.5$, $n_2 = 1$, $n_3 = 1.7 - 0.008i$, and $n_4 = 4.7 - 0.2i$ respectively. At the right and left boundaries of the simulation model, periodic boundary conditions were introduced. This virtually represents an infinitely wide simulation area. At the top and bottom boundaries, no boundary conditions were introduced, because the calculation terminated when light reached the top boundary. Note that no light reaches the bottom boundary because of the opaque silicon substrate.

A plane wave light source with a wavelength of $\lambda = 442$ nm is located at the band of $z = 1.45 - 1.89$ μm in the mold, as shown in Fig. 2. This band-shaped light source moderates the change of light intensity within/around the light source, reducing its noise. A 1.5 μm gap between the light source and the mold surface reduces noise from the light source to the mold surface. The light source emits light at an incident angle, ϕ, which satisfies total internal reflection condition, $\phi > \arcsin(n_2/n_1) = 41.8°$. The incident angle also satisfies $\phi = \arcsin(m\lambda/n_1 w_x)$, which produces light with the same phase at the right and left boundaries of the light source to meet the periodic boundary conditions. In this
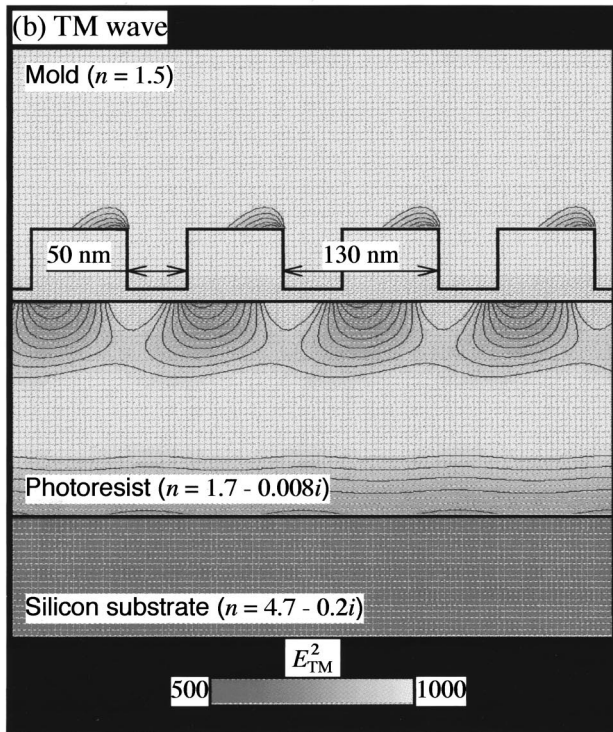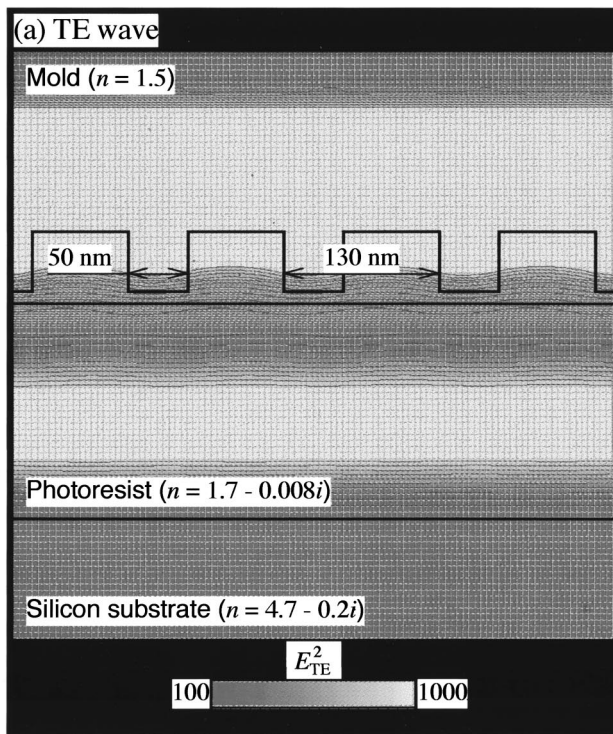
FIG. 3. Distribution of optical near-field intensity obtained with an air gap of 10 nm. TE and TM polarization were used in panels (a) and (b), respectively.

FIG. 4. Distribution of optical near-field intensity obtained using TM-polarized light without an air gap.

equation, m and w_x represent a natural number and the x-directional width of the simulation model respectively.

Cell sizes, depending on its location in the simulation model, vary in the range of 2–20 nm, which is much smaller than both the exposure light wavelength and the microrelief feature on the mold. The time step, 6×10^{-18} s, satisfies
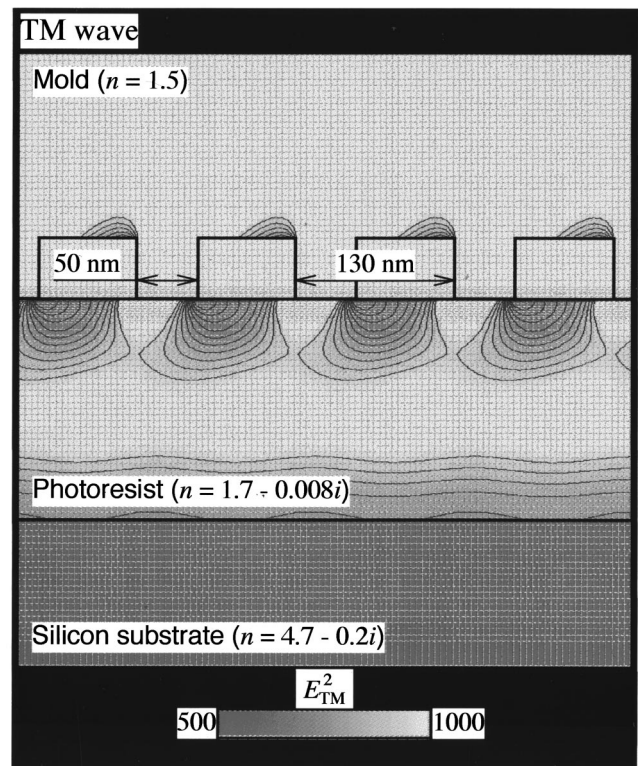
Courant condition with only a small margin. The number of calculated steps was approximately 2×10^3, in which the amplitude of an electric field reached steady state.

IV. CALCULATION RESULTS AND COMPARISON WITH EXPERIMENTS

We first performed simulation using the mold with 130 nm pitch grating protrusions of 50 nm in height and width. A photoresist film was 180 nm in thickness through all simulations. Figure 3 shows the distribution of optical near-field intensity obtained when an air gap was 10 nm, where TE and TM polarization were used in panels (a) and (b), respectively, (TE and TM polarization are defined in Fig. 2). In this figure, curved lines represent the contours of optical near-field intensity, and color bar indicators linearly show the optical near-field intensity relative to the light source intensity defined as 1000.

Figure 3 confirms clear difference on the distribution of optical near-field intensity between TE polarization (a) and TM polarization (b). In the case of TM polarization, optical near-field intensity from the surface to several tens of nanometers deep inside of the photoresist film distributes according to the grating protrusions on the mold. In the case of TE polarization, in contrast, the distribution is nearly uniform. This is because the electric field vector of TM polarization is perpendicular to the running direction of the linear protrusions on the mold, whereas that of TE polarization is parallel. Similar dependence of the optical near-field intensity distribution on the exposure light polarization has been confirmed in other near-field photolithography.[2–5]
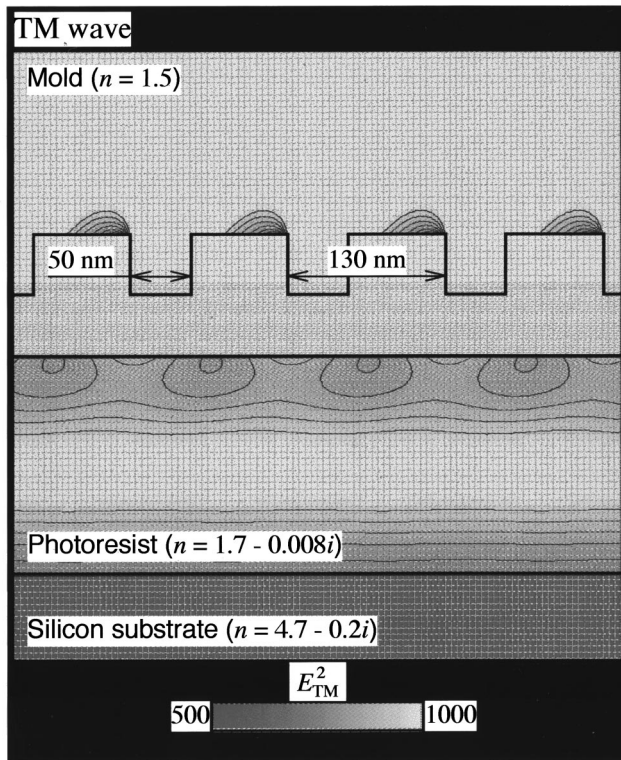
FIG. 5. Distribution of optical near-field intensity obtained using TM-polarized light with a 50 nm air gap.

FIG. 7. Scanning electron micrographs of patterned positive photoresist films. The photoresist films shown in panels (a) and (b) were exposed to TE- and TM-polarized light, respectively, using the replica mold shown in Fig. 6.

Next, we changed the air gap from 10 to 0 and 50 nm. Figures 4 and 5 show the distribution of optical near-field intensity in cases of 0 and 50 nm air gap setting, respectively. Note that the uniform distribution in case of TE polarization, like in Fig. 3 (a), is omitted. Comparing Figs. 4, 3(b), and 5 demonstrates that the contrast of optical near-field intensity in the photoresist film reduces as the air gap increases. This suggests the advantage of close contact between the mold and the photoresist film.

As well known, the resolution of projection photolithography is limited by the diffraction limit of light, $\lambda/(2n\mathrm{NA})$, where NA is the numerical aperture. In our near-field photolithography, the diffraction limit of light is approximately 150 nm with $\lambda = 442$ nm, $n = n_1 = 1.5$, and NA$\rightarrow$1. These simulation results indicate that near-field photolithography can potentially resolve a 130 nm pitch grating pattern finer than the diffraction limit of light.

The earlier-mentioned simulation results, however, shows poor agreement with experimental results. Figure 6 shows an acetyl cellulose replica mold. Figures 7(a) and 7(b) show positive photoresist films which were exposed to TE- and TM-polarized light, respectively, using the replica mold shown in Fig. 6. The photoresist film was 180 nm in thickness as it was in the simulation model. Exposure light was incident perpendicularly to ridges on the replica mold, that is, grooves on the photoresist film. We have already reported the experimental method and setup in another paper.[9]

As Fig. 7 shows, the photoresist film exposed to TE-polarized light (a) had four pairs of grooves transferred from the microrelief on the replica mold, whereas that exposed to
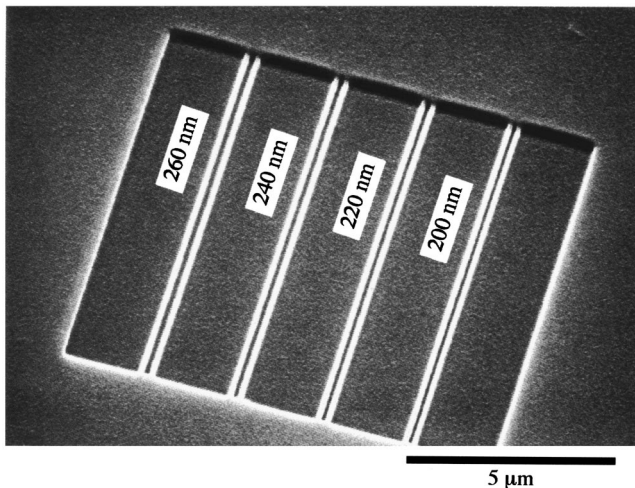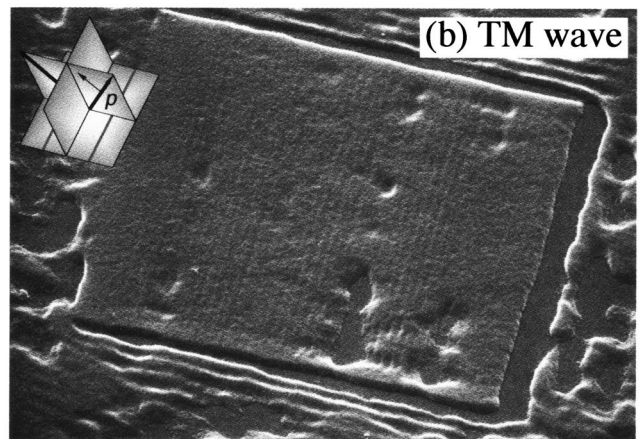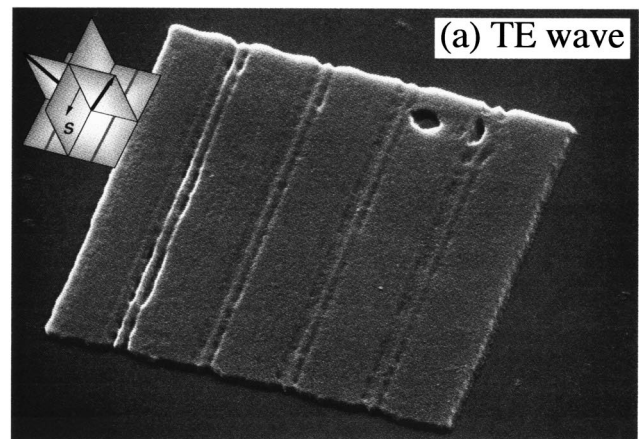

FIG. 6. Scanning electron micrograph of an acetyl cellulose replica mold. The groove pairs with a width of 70 nm show pitches of 200, 220, 240, and 260 nm from the right.
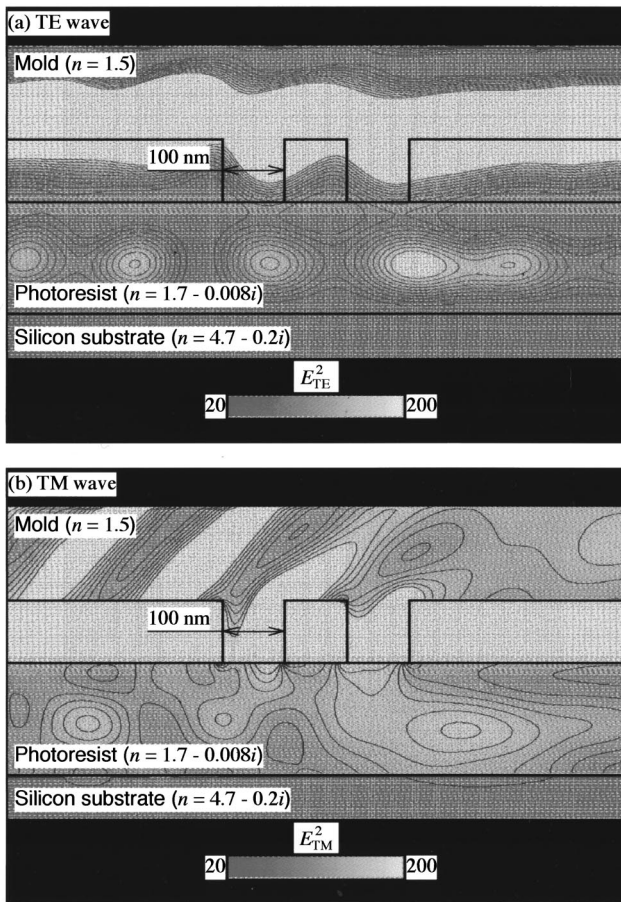
FIG. 8. Distribution of optical near-field intensity obtained without an air gap. TE and TM polarization were used in panels (a) and (b), respectively.
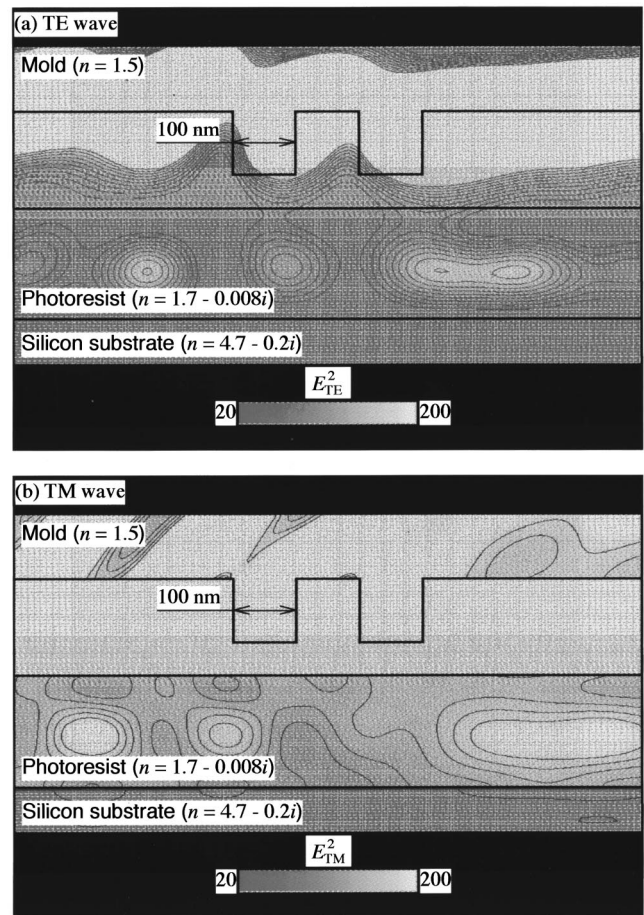

FIG. 9. Distribution of optical near-field intensity obtained with a 50 nm air gap. TE and TM polarization were used in panels (a) and (b), respectively.

TM-polarized light (b) had only an interferometric grating and not the pattern expected from the microrelief. These experimental results contradict with the earlier-mentioned FDTD simulation results in terms of the relation between polarization and pattern transferability.

We then conducted additional FDTD simulation using a model which better matched the experimental condition, instead of using the grating mold which was different from that used in the experiments. In the following simulation, we changed the grating pattern on the mold into one pair of ridges.

Figure 8 shows the distribution of optical near-field intensity obtained when the mold and the photoresist film were in contact with each other, and Fig. 9 shows that obtained when the air gap was 50 nm. Panels (a) and (b) in these figures are the simulation results in cases of TE and TM polarization, respectively, like those in Figs. 3–5. The distribution of optical near-field intensity in the photoresist films is apparently complicated and different from the earlier-mentioned simulation results obtained with the grating mold. Now we consider patterns expected to be fabricated on a photoresist film, assuming that a positive photoresist film is developed only down to several tens of nanometers depth from the surface. Note that this assumption does not contradict the experimental method. When exposed positive photoresist films were completely developed, the large parts of the

photoresist films were removed from the substrates. This can be predicted from Figs. 8 and 9 showing strong light intensity deep in the photoresist films.

On the photoresist film exposed to TE-polarized light, two grooves with different widths are expected from Figs. 8(a) and 9(a). On the photoresist film exposed to TM-polarized light in contact with the mold, two grooves with different widths as well as an interferometric grating pattern running to light incidence side are expected from Fig. 8(b). On the photoresist film exposed to TM-polarized light with the 50 nm air gap, only an interferometric grating pattern running to light incidence side is expected from Fig. 9(b).

Comparing the simulation results with the experimental results under the earlier-mentioned assumption, the simulation results shown in Fig. 9 fairly agree with the experimental results shown in Fig. 7; the photoresist film exposed to TE-polarized light showed two grooves with different widths and that exposed to TM-polarized light showed the interferometric grating as the simulation predicted. The experimental results agree better with the simulation result shown in Fig. 9 than that shown in Fig. 8 in the case of TM polarization. This indicates that there was an air gap of about 50 nm between the mold and the photoresist film during exposure. The air gap could be caused by a low height of the ridge pairs compared to that of the mesa surrounding the ridges on the replica mold shown in Fig. 6.
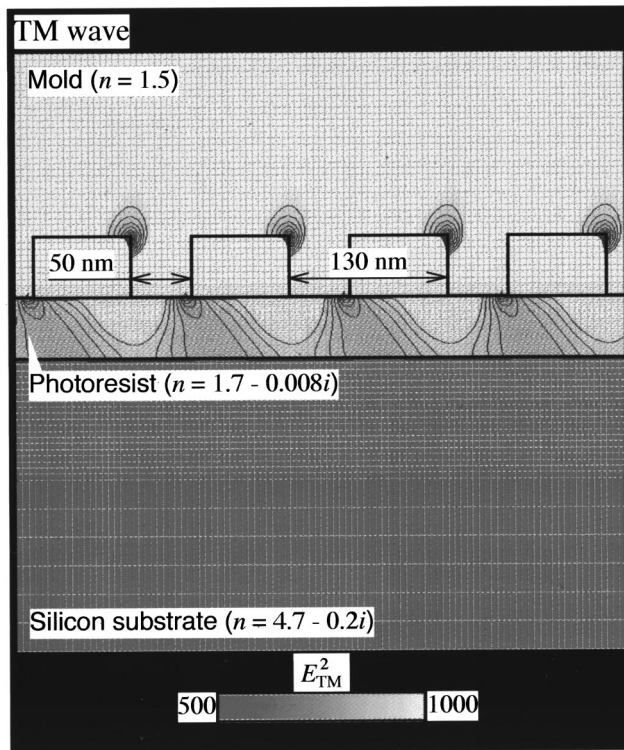
FIG. 10. Distribution of optical near-field intensity in the 50-nm-thick photoresist film exposed to TM-polarized light without an air gap.

FIG. 11. Distribution of optical near-field intensity in the photoresist film with a refractive index of $1.7-0.1165i$. TM-polarized light was used for exposure.

V. DISCUSSION

Our FDTD simulation results fairly agreed with our experimental results. This proves that our FDTD simulation of an optical near-field is useful for predicting exposure results. This FDTD simulation is especially essential for designing microreliefs on molds, because patterns fabricated on photoresist films sometimes differ from the microrelief patterns on molds.

We applied FDTD simulation to predict exposure results obtained when photoresist films with different thicknesses and refractive indices were used. The first FDTD simulation used a thinner photoresist film. Both the FDTD simulation and experiment showed that evanescent light generates only in the near field of the mold surface, and transfers the microrelief features on the molds only to the thin surface layers of the photoresist films. Thus, the photoresist film has to be as thin as the smallest microrelief feature to completely resolve through the photoresist film thickness. Figure 10 shows the simulation result obtained with a 50-nm-thick photoresist film. This figure does not show the uniform distribution of optical near-field intensity in the case of TE polarization. This figure indicates that a 130 nm pitch grating pattern, which is finer than the diffraction limit of light, can be completely resolved through the entire 50 nm thickness of the photoresist film. Combining the near-field photolithography using a sufficiently thin photoresist film with multilayer resist methods[10,11] would allow us to produce a resist mask thick enough for the following process like etching and lift-off.

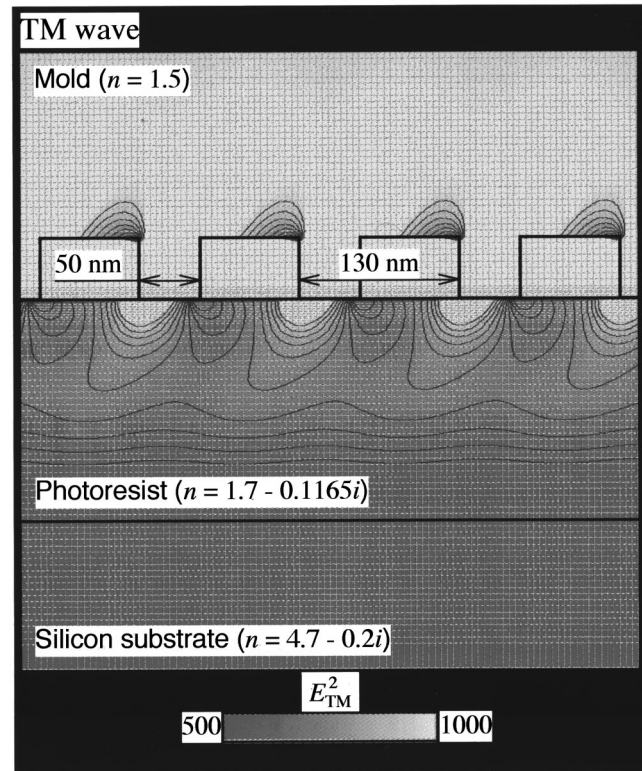Next, we varied the refractive index of the photoresist film. Other conditions were kept the same as those for the previous simulation shown in Fig. 4. Figure 11 shows the simulation result obtained when the refractive index of a photoresist film was set at $n_3 = 1.7 - 0.1165i$. This refractive index represents one hundredth of the original transparency. The result indicates that the smaller transparency localizes an exposed area in the surface layer of the photoresist film, improving the exposure contrast in the surface layer. Figure 12 shows the simulation result obtained when the refractive index of a photoresist film was set at $n_3 = 1.5 - 0.008i$, a refractive index with a smaller real part compared to the original one. The result shows deeper penetration of light from the mold into the photoresist film improving the exposure contrast in the surface layer again. Other papers[12,13] have reported that surface imaging technology can dry develop a photoresist film whose exposed area is confined in the surface layer for the next-generation photolithography. If we apply such surface imaging technology to the near-field photolithography, we can completely resolve photoresist films exposed like in Figs. 11 and 12 through the entire thickness of the thick photoresist film.

VI. CONCLUSION

Near-field photolithography uses evanescent light generated on a transparent mold by illumination under total internal reflection condition. We simulated its exposure in two dimensions using the FDTD method. The simulation results confirmed that the near-field photolithography can resolve a 130 nm pitch grating pattern, which is finer than the diffraction limit of light. They also confirmed the strong influence
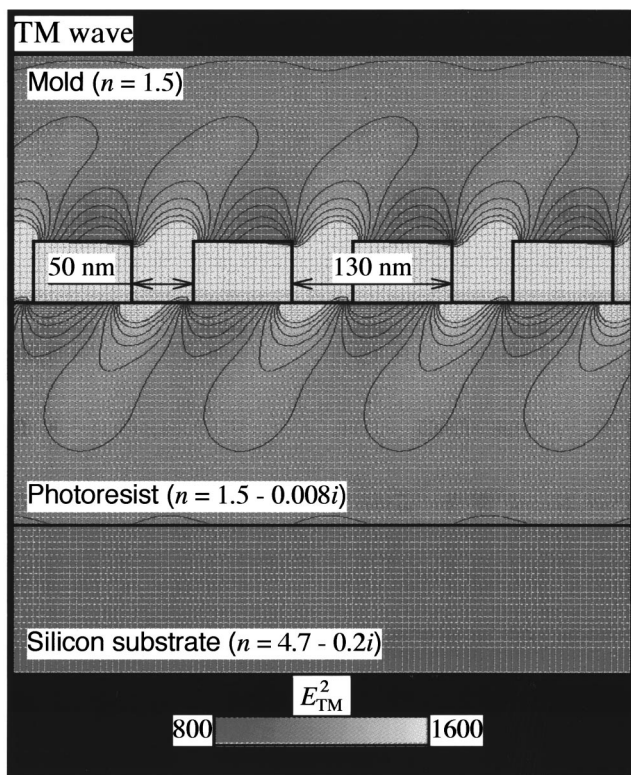
FIG. 12. Distribution of optical near-field intensity in the photoresist film with a refractive index of $1.5 - 0.008i$. TM-polarized light was used for exposure.

of exposure light polarization to the optical near-field distribution in a photoresist film, and showed their fair agreement with experimental results. FDTD simulation is, thus, a promising method to predict exposure results for designing molds.

The near-field photolithography has the problem that it exposes only the thin surface layer of a photoresist film to evanescent light localizing in the near field of the photoresist surface. Based on our simulation results showing the good exposure contrast in the photoresist surface, we suggested two solutions to this problem: the multilayer resist method which allows us to use a sufficiently thin photoresist film, and the surface imaging technology which can completely dry develop a thick photoresist film even if its exposure area is confined in the surface layer.

[1] Y. Mitsuoka, K. Nakajima, and T. Sakuhara, T. IEE Japan **120-E**, 52 (2000) (in Japanese).
[2] T. Ono and M. Esashi, Jpn. J. Appl. Phys., Part 1 **37**, 6745 (1998).
[3] M. M. Alkaisi, R. J. Blaikie, S. J. McNab, R. Cheung, and D. R. S. Cumming, Appl. Phys. Lett. **75**, 3560 (1999).
[4] J. G. Goodberlet, Appl. Phys. Lett. **76**, 667 (2000).
[5] S. J. McNab and R. J. Blaikie, Appl. Opt. **39**, 20 (2000).
[6] J. A. Rogers, K. E. Paul, R. J. Jackman, and G. M. Whitesides, Appl. Phys. Lett. **70**, 2658 (1997).
[7] H. Schmid, H. Biebuyck, B. Michel, and O. J. F. Martin, Appl. Phys. Lett. **72**, 2379 (1998).
[8] L. P. Ghislain, V. B. Elings, K. B. Crozier, S. R. Manalis, S. C. Minne, K. Wilder, G. S. Kino, and C. F. Quate, Appl. Phys. Lett. **74**, 501 (1999).
[9] S. Tanaka, M. Nakao, Y. Hatamura, M. Komuro, H. Hiroshima, and M. Hatakeyama, Jpn. J. Appl. Phys., Part 1 **37**, 6739 (1998).
[10] K. Tsuji, M. Sasago, and K. Kugimiya, IEEE Trans. Electron Devices **ED-31**, 1861 (1984).
[11] J. M. Moran and D. Maydan, J. Vac. Sci. Technol. **16**, 1620 (1979).
[12] N. Matsuzawa, S. Mori, M. Endo, T. Mirisawa, Y. Kaimoto, K. Kuhara, and M. Sasago, J. Photopolym. Sci. Technol. **11**, 625 (1998).
[13] S. Mori, K. Kuhara, T. Morisawa, N. Matsuzawa, Y. Kaimoto, M. Endo, T. Matsuo, and M. Sasago, Jpn. J. Appl. Phys., Part 1 **37**, 6734 (1998).